

2006

Two-Phase Refrigerant Distribution in a Micro-Channel Manifold

Chad D. Bowers

University of Illinois at Urbana-Champaign

Predrag Hrnjak

University of Illinois at Urbana-Champaign

Ty Newell

University of Illinois at Urbana-Champaign

Follow this and additional works at: <http://docs.lib.purdue.edu/iracc>

Bowers, Chad D.; Hrnjak, Predrag; and Newell, Ty, "Two-Phase Refrigerant Distribution in a Micro-Channel Manifold" (2006).
International Refrigeration and Air Conditioning Conference. Paper 743.
<http://docs.lib.purdue.edu/iracc/743>

This document has been made available through Purdue e-Pubs, a service of the Purdue University Libraries. Please contact epubs@purdue.edu for additional information.

Complete proceedings may be acquired in print and on CD-ROM directly from the Ray W. Herrick Laboratories at <https://engineering.purdue.edu/Herrick/Events/orderlit.html>

Two-Phase Refrigerant Distribution in a Micro-Channel Manifold

Chad D. BOWERS, Predrag S. HRNJAK¹, Ty A. NEWELL²

Department of Mechanical and Industrial Engineering
University of Illinois at Urbana-Champaign
1206 W. Green St., Urbana, IL 61801, USA
¹(pega@uiuc.edu) ²(tynewell@uiuc.edu)

ABSTRACT

This paper presents an experimental investigation of two phase flow distribution in a micro-channel manifold. This horizontally oriented, transparent manifold (ID=20mm) distributed two-phase refrigerant to a linear array of 15 micro-channels. Flow through the micro-channels was in the downward direction. To better understand the governing factors of distribution within the manifold, both geometrical considerations (micro-channel protrusion and into the manifold length from expansion device) and flow characteristics (inlet quality and mass flux) were considered. Refrigerant R134a was used as a working fluid.

1. INTRODUCTION

Heat exchanger efficiency is strongly influenced by the distribution of the refrigerant within the heat exchanger. Dry out of channels, due to poor liquid refrigerant distribution, can cause dramatic decrease of heat capacity in the effected channels of an evaporator. With that in mind, the primary objective of this project is to gain a better understanding of the parameters governing the distribution of two-phase refrigerant flow, with special emphasis on liquid distribution, in a generic micro-channel manifold. This was done using experiments run in a test section manifold with fifteen micro-channels set in a linear array. This generic manifold is similar in scale to a small capacity automotive heat exchanger. Similar projects investigating distribution characteristics of air/water and R134a have been conducted. Fei (2004) conducted an investigation into R134a distribution in a generic rectangular manifold. Air/water investigations using a rectangular manifold similar in scale to the current manifold with flush mounted micro-channels were conducted by Tompkins *et al.* (2002) and Yoo *et al.* (2002). Another air/water investigation of manifolds was done by Lee and Lee (2004), in which tube intrusion effects were studied in a vertically oriented manifold. A previous R-134a investigation using a manifold much like the one used in Tompkins and Yoo's work, with the micro-channels mounted flush in the manifold was conducted by Zhang *et al.* (2004). Vist and Petersen (2004) studied two phase flow distribution in a horizontally oriented circular manifold feeding 10 parallel 4mm tubes with R-134a. While many studies of distribution have been conducted, it seems (to the best of the authors' knowledge) that none using both a circular manifold, similar to those found in real heat exchangers and actual micro-channels has been conducted in conjunction with R-134a being used as the working fluid.

2. EXPERIMENTAL FACILITIES

The manifold test section used in this experiment was installed in the refrigerant loop shown in Figure 1. A single-phase pump is used to obtain the desired mass flow rate of R-134a through the loop. The mass flow rate and density is measured by a coriolis mass flow meter ($\pm 0.10\%$). The inlet pressure of the manifold is controlled by a needle expansion valve placed near the inlet of the manifold. Inlet quality is controlled by an electric heater and is calculated using system pressures and temperatures and checked by measurement of liquid flow rates. The two system pressures measured were the inlet pressure (before the expansion device) and outlet pressure (after the manifold). These pressures varied from 0.8 MPa to 2.9 MPa and 600 kPa to 760 kPa, respectively. Pressure transducers (± 0.7 kPa) placed before and after the test section displayed these pressures. System temperatures were displayed in a similar manner using thermocouples (the greater of $\pm 0.5^\circ\text{C}$ or $\pm 0.4\%$) placed before and after the test section. Inlet temperatures varied from 22°C to 65°C , while outlet temperatures were maintained at room

temperature ($\sim 22^{\circ}\text{C}$). Liquid flow rates through the micro-channels were measured using a series of five cylinders in which liquid and vapor are separated with the mass of liquid gathered during a given amount of time being measured, thus yielding a time averaged liquid mass flow rate for five groups of three micro-channels. The grouping of the micro-channels along with the collection cylinders can be seen schematically in Figure 1.

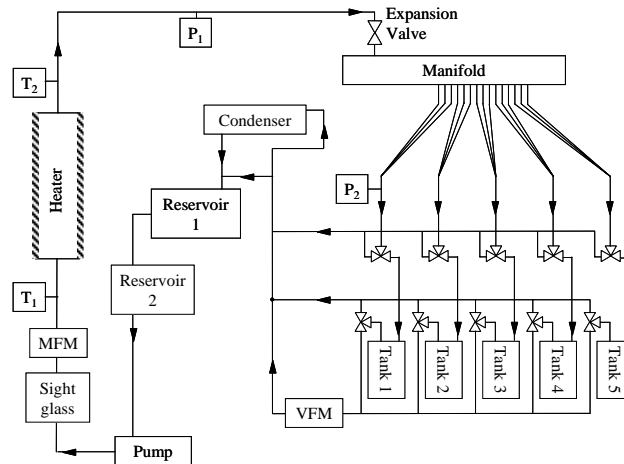


Figure 1: Experimental Facility

3. MICRO-CHANNEL MANIFOLD DESCRIPTION

In order to represent more realistically a real heat exchanger manifold, a circular micro-channel manifold was designed and constructed. The manifold consists of three main components: a view plate, a micro-channel mounting plate, and the manifold tube. The view plate and the mounting plate both have exterior dimensions of 101.6mm by 165.1mm. The view plate, shown in figure 2, is made of clear polycarbonate; while the mounting plate is made of aluminum. A manifold tube makes up the flow field of the manifold; this tube has an inner diameter of 20.42mm and a length of 482.6mm. The manifold tube is made of clear PVC and sealed between the view plate and the mounting plate. An array of slots for the micro-channels is machined into the tube so that the micro-channels can be protruded into the tube. This array is offset on the tube so that there are two different lengths between the inlet and the micro-channels. The two entrance lengths for the circular manifold are 267mm and 89mm from the micro-channel array respectively. The micro-channel tubes used are 6-port tubes with a hydraulic diameter of 1.54mm. For this experiment the length of the tubes is 317.5 mm. Sealing of the tubes is achieved by rubber o-rings placed in chamfered grooves on the micro-channel mounting plate

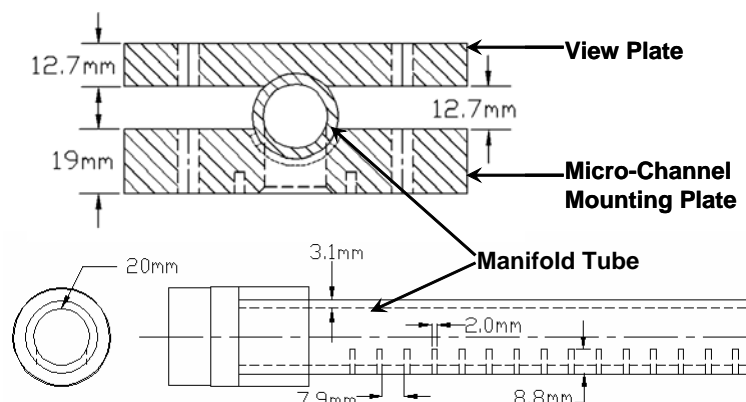


Figure 2: Micro-Channel Manifold Test Section

The array of micro-channels is protruded into the flow field to the desired protrusion depth. In order to seal properly, the micro-channels must be protruded to the point that the micro-channel entirely fills the machined slots in the manifold tube. This results in the micro-channels being protruded nearly one quarter of the diameter of the

tube, or 5.6mm. This particular protrusion scheme is very similar to the protrusion of micro-channels in a real heat exchanger. The two other uniform protrusion depths studied have the micro-channels protruded half the diameter of the tube and to the point where the micro-channels hit the upper wall of the tube; this is nearly three-quarters of the diameter. These depths are 10.2mm and 14.7mm respectively. The three protrusion schemes described above are designated “1/4”, “1/2”, and “3/4” respectively. Two additional micro-channel protrusion cases were studied using this manifold. These cases consisted of two separate methods of staggering the depth of the micro-channel protrusion as they progressed through the manifold. The array was staggered from 5.6mm into the manifold to 14.7mm into the manifold (or from “1/4” depth to “3/4” depth), for one case and in the reverse direction for the other. These protrusion schemes were designated as stagger up (SU) and stagger down (SD) respectively. The five different protrusion schemes are shown in Figure 3.

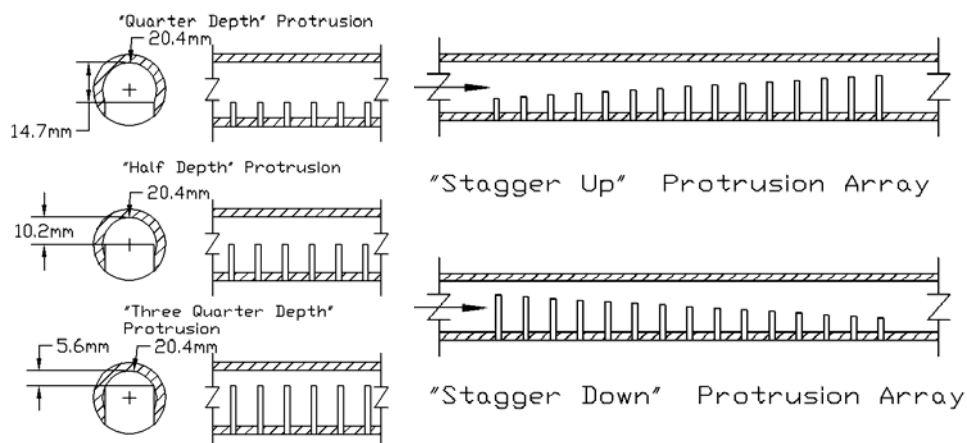


Figure 3: Micro-Channel Protrusion Scheme

4. EXPERIMENTAL PARAMETERS

Both geometric and dynamic parameters were considered in this experiment. The geometric parameters, micro-channels protrusion and entrance length, were described in some detail above. The inlet flow parameters studied were the mass flow rate and the inlet quality. Inlet quality was varied from 0% to 35%, and the mass flow rate was varied from 15g/s to 35 g/s. These mass flow rates yielded inlet mass fluxes in the manifold that ranged from 46 to 107 kg/m²-s. Inlet flow conditions coupled with protrusion depth and entrance length as well as the system limitations led to 310 possible test cases with 306 actually being performed.

5. RESULTS AND DISCUSSION

5.1 Distribution Results – Short Entrance

The distribution results for all five protrusion schemes at a given inlet condition ($x=15\%$, $G=76$ kg/m²s) are presented in Figure 4. The fraction of total liquid mass flow rate is plotted on the ordinate and the collection tank that sees that flow on the abscissa. Figure 4 shows how little varying the protrusion depth or scheme affects the distribution trends, when the fluid is expanded close to the micro-channel array. For all cases, except the stagger up protrusion scheme, the first and the last collection tank receive the least amount of flow while the middle tank receives the most. However, the distribution is relatively uniform, especially when compared to the results for the cases in which the fluid is expanded further from the micro-channel array, as will be seen later.

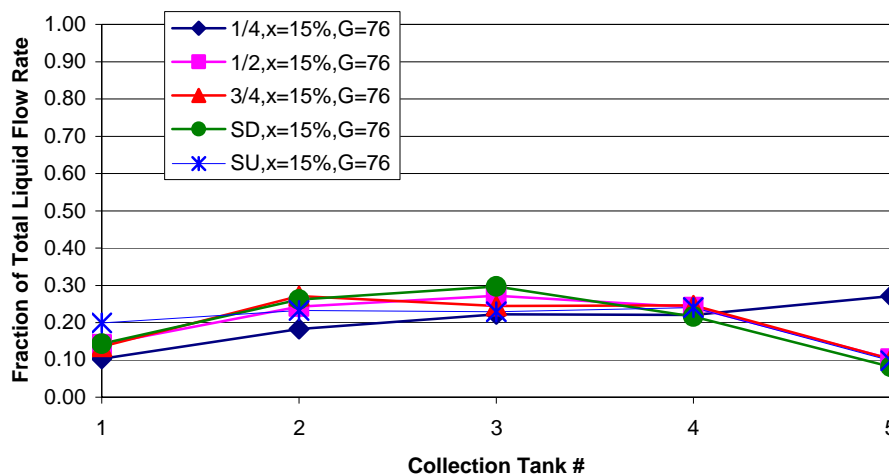


Figure 4: Distribution Results for Short Inlet Case ($x=15\%$ & $G=76\text{kg/m}^2\text{s}$)

In order to better evaluate the distribution results they will be presented in terms of a coefficient of variation. The coefficient of variation (CV) is a measure of relative scatter with respect to the mean. Here the mean is considered to be exactly uniform liquid distribution (i.e. all the collection tanks receive the same liquid flow rate). Thus, for present concerns the CV measures how far the liquid flow distribution deviates from completely uniform distribution. The use of the coefficient of variation allows the five points relating to liquid flow in each collection tank to be reduced to one point that tells how uniformly the flow is distributed. This allows for a more compact analysis of the effect of varying test parameters. Equation (1) shows the equation used to obtain the CV. Where the standard deviation is gained from Equation (2) and the mean liquid mass flow rate is defined as shown in Equation (3). The CV is bounded by 0 and 2. The boundary value of 0 represents completely uniform distribution while the boundary value of 2 represents the entire liquid flow rate entering only 1 collection tank. It should be noted that the simplicity gained by using the CV as a measure of the uniformity of the distribution leads to a loss of information regarding where the maldistribution occurs within the manifold. In other words, the flow could be distributed to one side of the manifold and yield a specific value of CV that could also be obtained from an equally maldistributed flow on the opposite side of the manifold.

$$CV = \frac{\sigma}{\bar{m}} \quad (1)$$

$$\sigma = \sqrt{\sum_{i=1}^n (\dot{m}_i - \bar{m})^2 / n} \quad (2)$$

$$\bar{m} = \frac{\sum_{i=1}^n \dot{m}_i}{n} \quad (3)$$

Now that a measurement of the uniformity of the liquid distribution has been constructed, trends based upon varying inlet and geometrical conditions can be examined. Figure 5 illustrates some of these effects for the short entrance case by comparing the CV against inlet mass flux and inlet quality. The graph on the left of Figure 5 shows the effect of changing inlet mass flux for a constant inlet quality (15%). This shows that there is little change in liquid flow distribution as the inlet mass flux increases, this trend holds for all the protrusion depths, with the exception of the stagger down case. The stagger down case has slightly less uniform distribution for the lowest two inlet mass fluxes. There is also very little effect of protrusion in these cases. The graph on the right of Figure 5 shows how the inlet quality influences liquid flow distribution, for a constant inlet mass flux ($61\text{kg/m}^2\text{s}$). Again, as seen by the flatness of the lines there is not a great deal of dependence on the inlet quality. It is interesting to note that while three quarter depth protrusion has relatively uniform distribution at lower inlet quality, the distribution actually

becomes less uniform as the inlet quality gets higher. The stagger down case again shows the least uniform of all protrusion schemes.

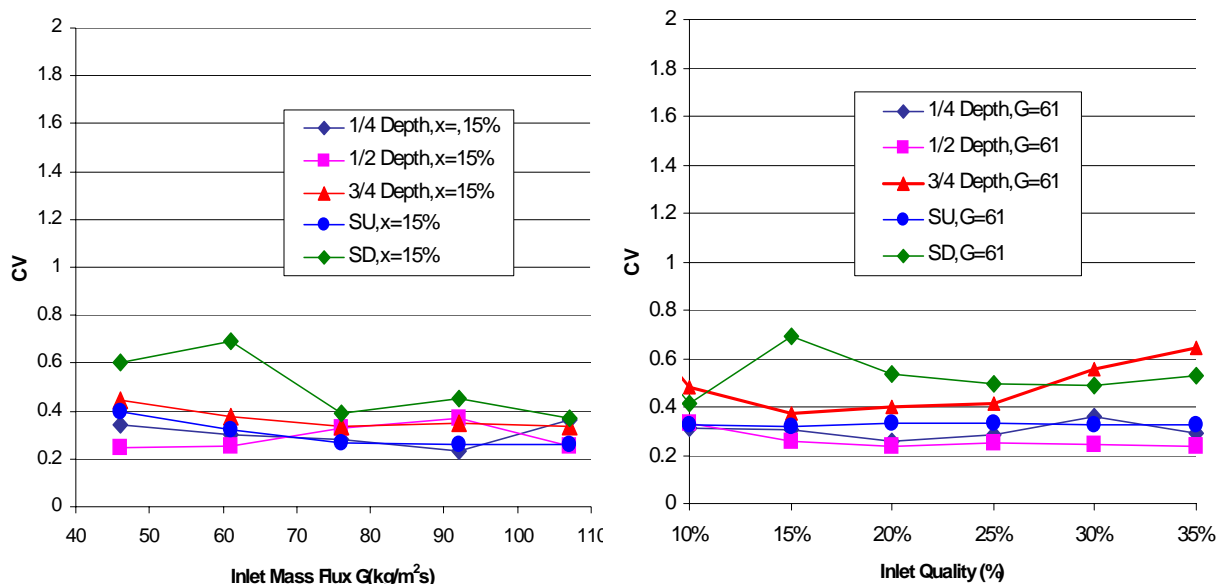


Figure 5: Effects of Mass Flux, Quality, and Protrusion on Distribution for Short Inlet Cases

5.2 Distribution Results – Long Entrance

The liquid flow distribution trends and their dependence on protrusion depth for the cases in which the fluid is expanded further from the micro-channel area are significantly different than those seen earlier for the short inlet cases. Figure 6 shows these trends for an inlet quality of 15% and mass flux of $76\text{kg/m}^2\text{s}$. The distribution starts off very poor for the “quarter depth” protrusion case, with the first two collection tanks seeing nearly all the liquid flow and the last three seeing dry-out or near dry out conditions. Liquid flow distribution improves slightly when the protrusion scheme is changed to the “half depth” and the “stagger down” schemes. Distribution is the most uniform for the “three quarter” depth protrusion case; the middle three tanks see close to the same amount of liquid flow while the first and last see less liquid flow rate, but no dry-out conditions appear.

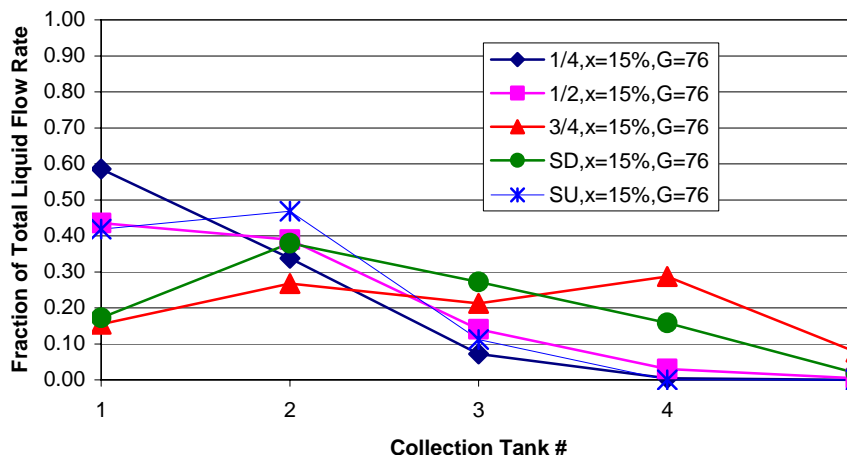


Figure 6: Distribution Results for Long Inlet Case ($x=15\%$ & $G=76\text{kg/m}^2\text{s}$)

Earlier, in Figure 5, it was seen how little inlet conditions (mass flux and quality) and micro-channel protrusion affect the distribution for the short entrance. Figure 7 shows how this is not the case when the fluid is expanded further from the micro-channel array. The graph on the left of Figure 7 shows how liquid distribution, for all

protrusion schemes, improves slightly as the inlet mass flux increases. It also shows how distribution also improves more dramatically for each increasing protrusion depth, with the three quarter depth protrusion having the most uniform liquid distribution over all mass fluxes. The graph on the right of Figure 7 shows that again, there is not a large influence of changing inlet quality over liquid flow distribution, but the dramatic effect of protrusion scheme is still seen. For the cases in which the flow entered through the inlet further from the micro-channel array protrusion has a significant effect, with increasing protrusion depth resulting in more uniform liquid flow distribution.

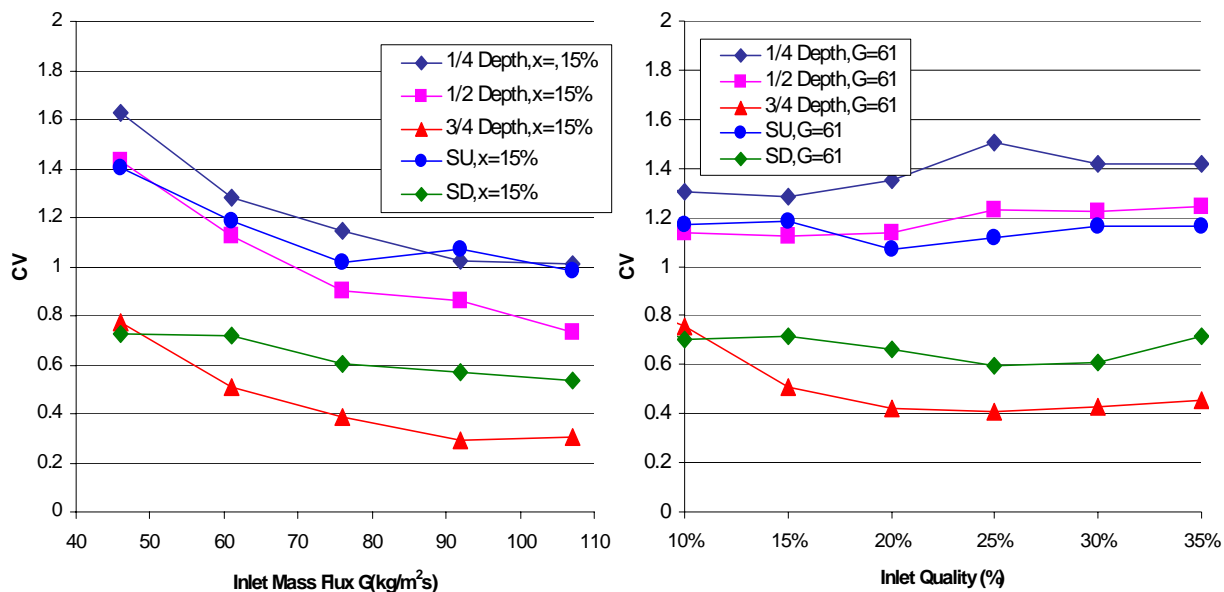


Figure 7: Effects of Mass Flux, Quality, and Protrusion on Distribution for Long Inlet Cases

5.3 Effective Mass Flux

It has been shown that there are slight dependences of liquid flow distribution on inlet quality and mass flux. More noticeable was the dramatic effect of improving distribution that protrusion scheme had. With all of these effects in mind it would be advantageous to have a parameter that combined the effects of protrusion depth, inlet quality, and mass flux. This will be done by using a parameter which will be referred to as the effective mass flux (G_{eff}). Inlet mass flux was calculated in the typical manner of dividing inlet mass flow rate by the cross sectional area of the manifold. In contrast, the effective mass flux was calculated by dividing the mass flow rate by the cross-sectional area above and around the micro-channel, as illustrated by the shaded area in Figure 8, and then multiplying that by one minus the quality. This essentially weights the mass flux that is seen at the first micro-channel by the mass fraction of liquid refrigerant. It should be noted that the effective mass flux for the staggered protrusion schemes was calculated using the cross-sectional area above and around the first micro-channel, so in the case of staggered-down the effective mass flux is the same as the three-quarter case.

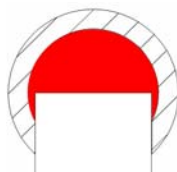


Figure 8: Area Used in Calculation of Effective Mass Flux (G_{eff})

How this effective mass flux influences distribution, for both the long and short inlets, can be seen in Figure 9. The left side of Figure 9 shows just how much the effective mass flux influences the liquid flow distribution when the flow comes from the longer entrance. At low effective mass fluxes the distribution is very non-uniform, but as effective mass flux increases liquid distribution becomes much more uniform. In contrast, the right side of Figure 9

shows how the short entrance cases behave with respect to effective mass flux. Even at lower effective mass fluxes, the value for CV is already relatively low; meaning that the liquid flow distribution is relatively uniform already. For the one quarter, half and stagger up protrusions the distribution becomes slightly more uniform as the effective mass flux increases. Then as the effective mass flux is increased by increasing the protrusion depth to the three quarter and stagger down schemes the value for CV increases, showing that the distribution actually becomes slightly less uniform. As the effective mass flux is increased by increasing mass flow rate for the three quarter and stagger down schemes liquid distribution begins to become more uniform again. This suggests that there is some sort of optimum protrusion scheme, at least for the short entrance cases. By comparing the left side of Figure 9 to the right side it is seen that the uniformity of the liquid distribution in the long entrance cases approaches the best uniformity achieved in the short entrance cases, but never quite reaches it. This suggests that the optimum protrusion scheme for the long inlet cases has not been achieved.

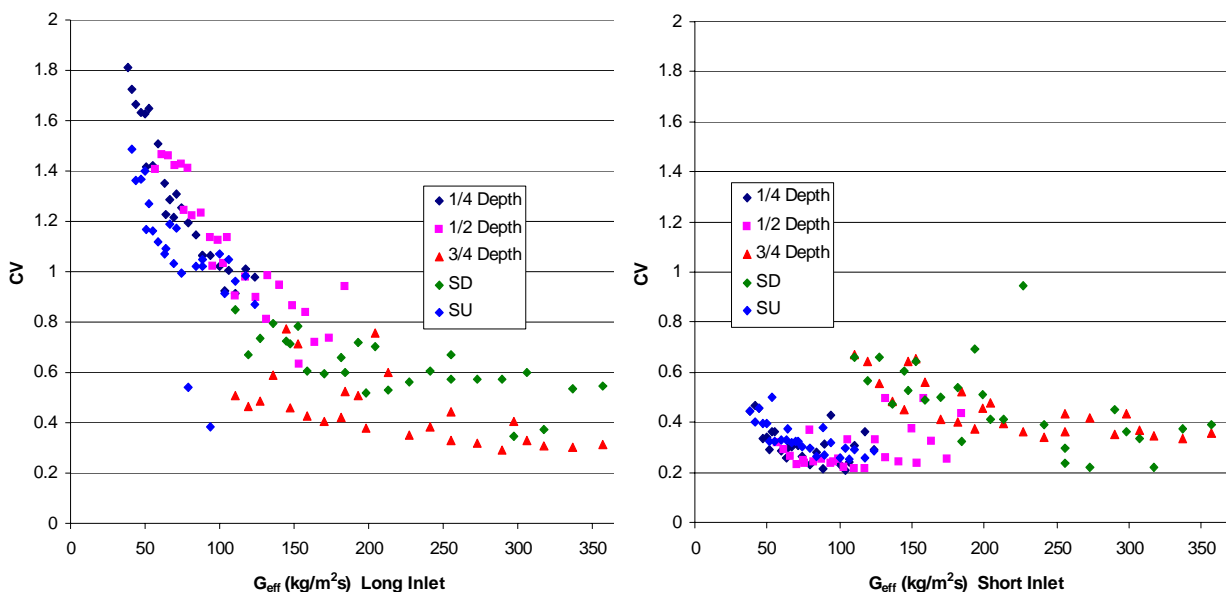


Figure 9: Effective Mass Flux Influence on Distribution

5.4 Flow Visualization Considerations

In conjunction with the above described distribution experiments, some flow visualization issues were studied as well. Visual study of the flow structures help to give some insight into why the distribution trends that are seen occurred. As the fluid exits the expansion device, the flow is very homogenous. When the expansion occurs close to the micro-channel array the two-phases stay homogenized and the distribution is relatively uniform. For the long inlet cases the two-phases of the flow separate before they reach the micro-channel array. When this separation is

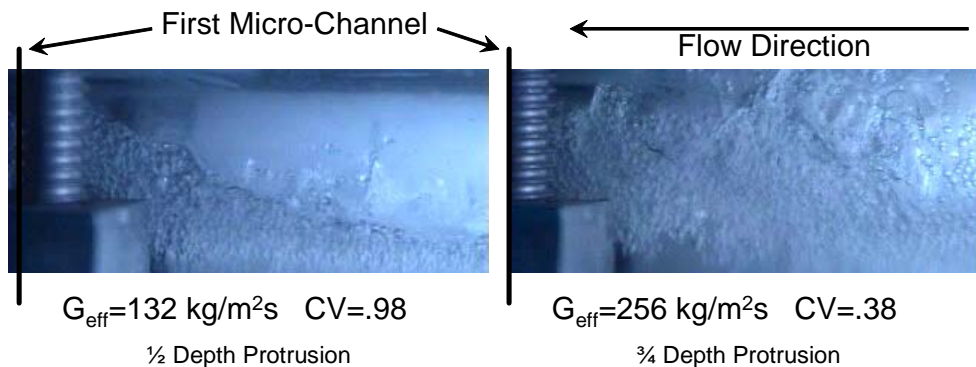


Figure 10: Flow Visualization for Long Entrance (approx. 250mm from expansion device)

maintained (in the cases of the smaller protrusion depths) the uniformity of liquid distribution is poor. The importance of avoiding this phase separation with regards to distribution has been noted by others, namely Zhang,

Lee and Lee, and Kulkarni *et al.* (2004). Improvement in distribution uniformity was seen when the deeper protruded micro-channels help to “re-homogenize” the two phases, entraining the liquid in the higher velocity vapor. This entrained liquid is then carried further down the manifold, yielding better distribution. An example of this separation and “re-homogenization” can be seen for the same inlet conditions ($x=10\%$, $m=25\text{g/s}$) in Figure 10. Phase separation is very apparent in the photo on the left which was taken, when the micro-channels were protruded to one half depth, whereas it is not seen on the right when protrusion depth is three quarters. While the difference in flow structure is striking, the difference in uniformity of distribution is also striking, as can be seen by the difference in CV values.

6. CONCLUSIONS

Liquid distribution within the micro-channel manifold depends upon several factors: the inlet mass flux, inlet quality, cross-sectional geometry and inlet entrance length. Generally, as the mass flux and protrusion depth increase the distribution becomes more uniform. The shorter inlet length provides the most consistently uniform distribution with an optimum protrusion depth near one half. The longer entrance seems to see more improvement from increasing the above stated parameters, most notably from micro-channel protrusion. The best uniformity of distribution occurred in the long entrance case when the micro-channels were protruded three-quarters into the manifold. These results show that for the best consistently uniform liquid distribution in a manifold of this sort it is desirable to expand the fluid as close to the manifold as possible. However, when this is not possible, there are ways that the uniformity of the liquid distribution can be improved, mainly by decreasing the area which the flow sees by micro-channel protrusion.

NOMENCLATURE

CV	coefficient of variation	(–)	Subscripts	
G	mass flux	($\text{kg/m}^2\text{s}$)	i	tank number
\dot{m}	mass flow rate	(g/s)	eff	effective
n	number of tanks	(–)		
σ	standard deviation	(g/s)		
x	quality	(%)		

REFERENCES

- Fei, P., Hrnjak, P.S., Newell, T.A., *Adiabatic Developing Two-Phase Flow Distribution in Manifolds of Heat Exchangers*,. Technical Report TR-225. Air Conditioning and Refrigeration Center, Univ. Illinois at Urbana-Champaign
- Kulkarni, T., Bullard, C., Keumnam, C., 2004, Header Design Tradeoff in Micro-channel Evaporators, *Applied Thermal Engineering*, 24 p. 759-776
- Lee, J. K., Lee, S. Y., 2004, Distribution of Two-Phase Annular Flow at Header-Channel Junctions, *Experimental Thermal and Fluid Science*, 28 p. 217-222
- Tompkins, D.M., Newell, T.A., Hrnjak, P.S., 2003. *Single Phase, Two-Phase Modeling; X-Ray Visualization for a Micro-Channel Manifold Distribution System*,. Technical Report TR-206. Air Conditioning and Refrigeration Center, Univ. Illinois at Urbana-Champaign
- Vist, S., Pettersen, J., Two-Phase Flow Distribution in Compact Heat Exchanger Manifolds, *Experimental Thermal and Fluid Science*, 28 p. 209-215
- Yoo, T., Hrnjak, P.S., Newell, T.A., *An Experimental Investigation of Two-Phase Flow Distribution in Micro-channel Manifolds*,. Technical Report TR-207. Air Conditioning and Refrigeration Center, Univ. Illinois at Urbana-Champaign
- Zhang, Q. M., Hrnjak, P.S., Newell, T.A., *An Experimental Investigation of R134a Flow Distribution in Horizontal Micro-channel Manifolds*,. Technical Report TR-223. Air Conditioning and Refrigeration Center, Univ. Illinois at Urbana-Champaign

ACKNOWLEDGEMENTS

International Refrigeration and Air Conditioning Conference at Purdue, July 17-20, 2006

Authors are grateful for the support of the ACRC at the University of Illinois at Urbana-Champaign